

FAST TRACK COMMUNICATION

Localization of inner-shell photoelectron emission and interatomic Coulombic decay in Ne₂

K Kreidi^{1,2}, T Jahnke¹, Th Weber³, T Havermeier¹, R E Grisenti^{1,4}, X Liu⁵, Y Morisita⁶, S Schössler¹, L Ph H Schmidt¹, M Schöffler¹, M Odenweller¹, N Neumann¹, L Foucar¹, J Titze¹, B Ulrich¹, F Sturm¹, C Stuck¹, R Wallauer¹, S Voss¹, I Lauter¹, H K Kim¹, M Rudloff¹, H Fukuzawa⁵, G Prümper⁵, N Saito⁶, K Ueda⁵, A Czasch¹, O Jagutzki¹, H Schmidt-Böcking¹, S K Semenov⁷, N A Cherepkov⁷ and R Dörner¹

¹ Institut für Kernphysik, J W Goethe Universität, Max-von-Laue-Str. 1, 60438 Frankfurt, Germany

² DESY, Notkestrasse 85, 22607 Hamburg, Germany

³ Lawrence Berkeley National Laboratory, Berkeley CA 94720, USA

⁴ Gesellschaft für Schwerionenforschung, Planckstr. 1, 64291 Darmstadt, Germany

⁵ Institute of Multidisciplinary Research for Advanced Materials, Tohoku University, Sendai 980-8577, Japan

⁶ National Metrology Institute of Japan, AIST, Tsukuba 305-8568, Japan

⁷ State University of Aerospace Instrumentation, 190000 St Petersburg, Russia

E-mail: doerner@atom.uni-frankfurt.de

Received 28 March 2008

Published 6 May 2008

Online at stacks.iop.org/JPhysB/41/101002

Abstract

We used cold target recoil ion momentum spectroscopy (COLTRIMS) to investigate the decay of Ne₂ after K-shell photoionization. The breakup into Ne¹⁺/Ne²⁺ shows interatomic Coulombic decay (ICD) occurring after a preceding atomic Auger decay. The molecular frame angular distributions of the photoelectron and the ICD electron show distinct, asymmetric features, which imply localization of the K-vacancy created at one of the two atomic sites of the Ne₂ and an emission of the ICD electron from a localized site. The experimental results are supported by calculations in the frozen core Hartree–Fock approach.

(Some figures in this article are in colour only in the electronic version)

Are inner-shell holes in homonuclear diatomic molecules localized at one of the atoms or delocalized over the two equivalent sites? This highly controversial question has been discussed in the literature for more than 35 years now (see, e.g. [1–11] and our discussion below). Here we report on an experiment answering that question for the Ne₂ van der Waals molecule. Intuitively strong arguments for both opinions may be found: the K-shell wavefunction is very tightly confined to the nuclei and the overlap between inner-shell orbitals at different atoms of a molecule is usually negligibly small [12]. Hence, the geometry of the problem suggests the idea of

individual localized atomic wavefunctions. The symmetry of the problem however suggests the opposite: both sites of the diatomic molecule are indistinguishable and therefore the total molecular wavefunction has to have well-defined *gerade* (g) or *ungerade* (u) symmetry. In order to construct the molecular many-body wavefunction it seems natural to employ only symmetry adapted single electron orbitals. A core level hole would then have well-defined g or u symmetry and hence be delocalized over the two sites. This approach is used in today's state-of-the-art theory concerning the photoionization and decay of Ne₂ [13].

To address this question of a possible localization in a quantum mechanically meaningful and experimentally accessible way one has to relate it to a measurable observable. A prime candidate is the energy of the state measured by photoelectron spectroscopy. Theoretical claims for core hole localization based on the energy date back to the classic works of Snyder [1] and Bagus [2]. They showed that allowing symmetry broken—i.e. localized—basis states for inner-shell vacancies in a Hartree–Fock calculation lowers the energy and yields better agreement with the experiment. It was later argued that this is a peculiarity of the Hartree–Fock approach [3]. More sophisticated present-day calculations on N_2 very well reproduce the experimentally observed energy splitting of about 100 meV between the $1\sigma_g$ and $1\sigma_u$ core-ionized states [4, 5]. This is generally taken as evidence for the delocalized character of the inner-shell hole.

As an alternative observable, sensitive to core hole localization, the angular distribution of the photoelectrons in the laboratory system was suggested [6]. Corresponding experiments on nitrogen molecules show good agreement with calculations using delocalized orbitals [7]. This conclusion is also supported by resonant soft x-ray emission experiments on O_2 [8]. There the parity selection rules indicate the symmetry and with it the delocalization of the core-excited state. In contrast to that, partial localization is shown in experiments on singly substituted $^{14,15}N_2$ [9]. Furthermore, experiments exciting an inner-shell electron inducing fast dissociation and observing the Auger electron emitted during this dissociation show a clear Doppler shift in the Auger peak. This proves that they are emitted from a localized source flying towards or away from the observer [10, 14].

In the present work we use an even more sophisticated probe for localization which is the electron angular distribution in the *body-fixed frame* of the molecule [14–16]: we investigate the angular distribution of a photoelectron and an electron emitted via interatomic Coulombic decay (ICD) [17] following Auger decay [18] for fixed molecular orientations. If the electron is emitted from a delocalized source its angular distribution will be symmetric with respect to the two atoms of the molecule (see, e.g. [19, 20]). If, however, it is emitted from one site, then the angular distribution can show a strong asymmetry due to interference of the electron wave that is multiply scattered in the molecular potential. For example, a strong forward focusing by the atomic neighbour can occur [21]. In a homonuclear diatomic molecule such an asymmetry however can only be observed for an asymmetric breakup of the molecule into two fragments of different charge which make the two ends of the molecule experimentally distinguishable. A first experiment along this line on N_2 found no asymmetry with respect to the N^{1+}/N^{2+} fragments [20]. Here we investigate the K-shell ionization of Ne_2 instead of N_2 for several reasons. First, K-shell ionized Ne_2 fragments into the asymmetric breakup channel Ne^{1+}/Ne^{2+} . Second, the K-shell radius of Ne_2 is 30 times smaller than the internuclear distance R of 5.86 au. The bond is purely van der Waals, the binding energy is only 3 meV and the g/u splitting is negligibly small compared to the natural line width. All this might make it plausible to think of Ne_2 as two neon atoms sitting close

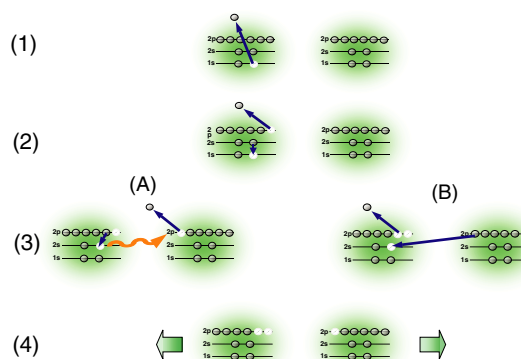


Figure 1. 1s photoionization (1) leads to an Auger decay resulting in a dicationic one-site state of Ne_2 (2). The Auger decay is followed by interatomic Coulombic decay (3) where the ion's excitation energy is emitted via a virtual photon transfer (A) or via electron transfer (B). Ending up in a state where both atoms are charged positively, the dimer fragments back-to-back in a Coulomb explosion (4).

together with their K-shells being independent of each other. Third however the opposing symmetry argument in favour of a delocalized description of all electrons by symmetry adapted wavefunctions of well-defined g or u parity is as valid for Ne_2 as it is for N_2 . Hence the key arguments keeping the question of possible localization open today in covalently bound molecules hold for van der Waals dimers, as well.

Santra *et al* [18] theoretically investigated the decay of Ne_2 after 1s ionization. They suggested that one-site Auger final states $Ne^{2+}(2s^{-1} 2p^{-1})/Ne$ decay further to a two-site state $Ne^{2+}(2p^{-2})/Ne^{1+}(2p^{-1})$ via ICD. Figure 1 shows a sketch of the different pathways of decay leading to this set of reaction products. Both decay routes start with K-shell ionization. In a localized scenario it is followed by an Auger decay of the same atom of the dimer yielding a vacancy in an inner valence shell ($Ne^{2+}(2s^{-1} 2p^{-1})/Ne$). Now two different channels of ICD may occur depending on the parity of the doubly charged states [22, 23]. Pathway (A) shows ICD via virtual photon exchange, (B) depicts the competing process involving the transfer of an electron. As both (A) and (B) lead to a triply charged species, Ne_2 fragments in a Coulomb explosion as a final step. The existence of ICD with its two centre nature is the key feature in Ne_2 , making it possible to trace core hole localization through all steps of the decay of Ne_2 . The sketch of the decay in figure 1 shows fully localized electrons and holes. Thus it may seem that the pure existence of ICD already proves a localization. This is not true however. While most discussions on ICD on an intuitive level use figures similar to our figure 1, all actual calculations on ICD, including the ones performed by Santra for the present system [18], work with molecular wavefunctions of well-defined g or u symmetry, i.e. they assume complete delocalization. The ICD calculations using symmetry adapted wavefunctions yield excellent agreement of the experimentally observed energies of the states and of the energy of the ICD electrons [13, 24]. These calculations report ICD electron energies separately for g and u symmetry again highlighting the delocalized character of the calculations [13].

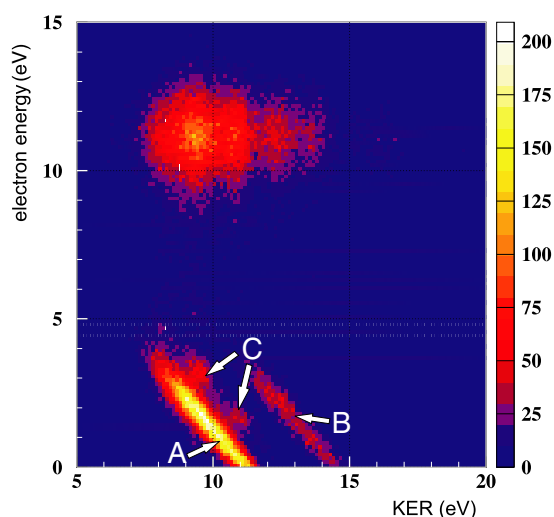


Figure 2. The kinetic energy of the ionic fragments in dependence of the electron energy. The photon energy is $h\nu = 881.2$ eV resulting in an energy of the $1s$ photoelectron of 11 eV. The two diagonal lines are a clear evidence for interatomic Coulombic decay (ICD). Line (A) is produced via the virtual photon exchange yielding a sum energy of 11.1 eV. Line (B) (with a sum energy of 14.3 eV) occurs as ICD via electron transfer happens. The origin of channel (C), showing two separate islands, is not quite clear.

The experiment was performed at beamline UE56/1-SGM of the Berlin Synchrotron (BESSY) using the COLTRIMS technique [25]. As a source for Ne_2 a supersonic jet that was precooled to 160 K was employed. It was crossed with the photon beam. Products from the photoreaction were guided by an electric field of 20 V cm^{-1} and a magnetic field of 6 Gauss towards two channel plate detectors with delayline readout [26]. Electrons up to 12 eV and ions up to 10 eV were detectable with a solid angle of 4π .

Figure 2 shows our experimental results for the measured electron energies and the sum of the kinetic energies of the ionic fragments (KER, kinetic energy release). With a photon energy of $h\nu = 881.2$ eV, events located at an electron energy of 11 eV correspond to photoelectrons from $\text{Ne } 1s$ ionization. Electrons originating from ICD are identified as diagonal lines (A) and (B). As the sum of the energy of the ionic fragments and the ICD electron is a constant, these diagonal lines with a slope of -45° are clear evidence for ICD as shown in [24].

The ICD channels, labelled (A) and (B) in figure 2, have a different KER which shows that the decay occurs at different internuclear distances. Similar to the findings in [23] both channels are created in an IC decay with the symmetry of the involved states and the difference in kinetic energy of the ions implying the occurrence of the two different contributions to ICD: channel (A) with a sum energy of 11.1 eV represents the decay from the inner valence excited one-site state $\text{Ne}^{2+}(2s^{-1}2p^{-1})[{}^1P]/\text{Ne}[{}^1S]$ to the two-site state $\text{Ne}^{2+}(2p^{-2})[{}^1D]/\text{Ne}^{1+}(2p^{-1})[{}^2P]$. This so-called ‘direct’ IC decay happens via an exchange of a virtual photon as sketched as pathway A in figure 1. The measured KER of ~ 8 eV to ~ 11 eV corresponds to an internuclear distance of ~ 3.6 Å to ~ 2.6 Å [27]. The mean value of this range is close to

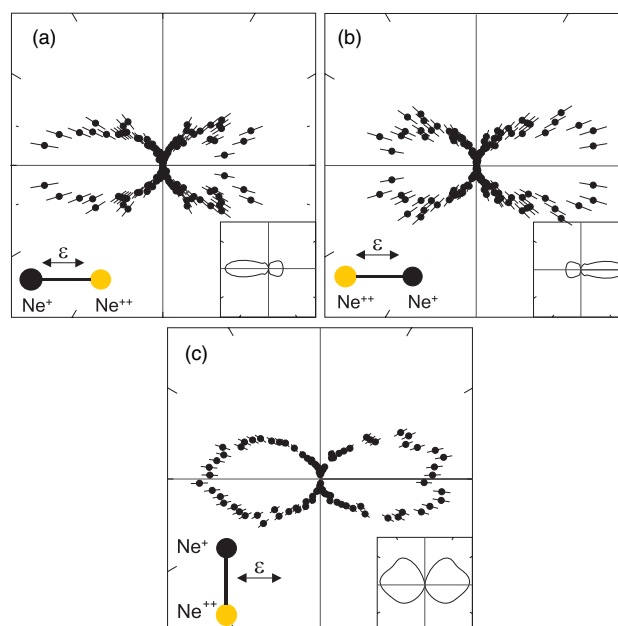


Figure 3. Angular distribution of the 11 eV $1s$ photoelectron in dependence of the orientation of the dimer axis and the direction of the polarization vector ε (horizontal). In (a) and (b) the dimer is aligned parallel to the polarization vector within an angle of $\pm 3^\circ$. In (c) the plane is defined by the dimer axis and the polarization of the light. The dimer is aligned perpendicularly to the polarization vector and the photoelectron is fixed relative to the plane within an angle of $\pm 10^\circ$. The asymmetry, being a result of core hole localization, is clearly visible in the experimental data (circles). Solid line: frozen core Hartree–Fock calculation assuming a localized emission.

3.05 Å which is the distance of the neon atoms in the ground state of Ne_2 and thus consistent with corresponding results in [23]. Channel (B) with a sum energy of $\text{KER} + \text{electron energy} = 14.3$ eV occurs at much higher KER (~ 11 eV to ~ 14 eV) which is equivalent to a internuclear distance of only ~ 2.6 Å to ~ 2.0 Å. Here the one-site state $\text{Ne}^{2+}(2s^{-1}2p^{-1})[{}^1P]/\text{Ne}[{}^1S]$ decays into the two-site state $\text{Ne}^{2+}(2p^{-2})[{}^3P]/\text{Ne}^{1+}(2p^{-1})[{}^2P]$ after electron transfer, as shown by pathway B in figure 1. The decay is described by the ‘exchange’ part of the electron–electron Coulomb matrix element. In this case the spatial overlap of the involved wavefunctions is the crucial contribution to the decay probability. Therefore pathway B is suppressed at large internuclear distances where pathway A is still open [23]. Beside channels A and B our experimental results also show two small islands, labelled as C in figure 2. The sum energy of $\text{KER} + \text{electron energy} = 12.1$ eV indicates the decay from the dicationic state $\text{Ne}^{2+}(2s^{-2})[{}^1S]/\text{Ne}[{}^1S]$ to the two-site state $\text{Ne}^{2+}(2s^{-1})(2p^{-1})[{}^3P]/\text{Ne}^{1+}(2p^{-1})[{}^2P]$. The KER of this decay is ~ 11 eV which is equivalent to $R = 2.6$ Å. This channel also represents a spin-flip ICD where electron transfer may play a role but until now it is not clear why it shows two separate islands instead of a complete diagonal line.

Figure 3 shows the angular distribution of the emitted photoelectron in the body fixed frame of Ne_2 . Clearly, the photoelectron angular distribution is asymmetric—the

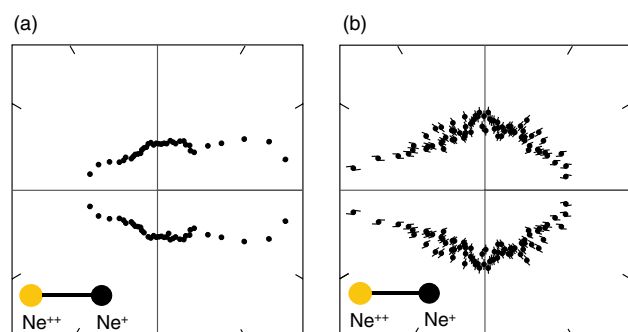


Figure 4. Angular distribution of the ICD electron in the dimer frame. The dimer is aligned horizontal and it is integrated over the orientation of the polarization vector. (a) ICD electrons which are created by virtual photon exchange (channel A in figure 1), (b) angular distribution of the ICD electrons emitted after transfer of an electron (channel B in figure 1). As suggested by the sketch in figure 1 the direction of the asymmetry switches from (a) to (b) depending on the decay path.

photoelectron is preferably emitted towards the singly charged dimer fragment. To validate our findings figures 3(a) and (b) show the results where the doubly charged ion is emitted in two opposite directions within the laboratory frame. As a support for our interpretation we compared the experimental angular distributions with a theoretical prediction for the case of a completely localized electron. The calculation was performed within the Hartree–Fock approximation using the method described in [28]: first the ground state of Ne_2 was computed in order to obtain the initial $1\sigma_g$ and $1\sigma_u$ wavefunctions. The photoelectron wavefunction was calculated in the frozen core Hartree–Fock approximation. Localization of the initial hole after photoionization on the right or left atom ($|r\rangle$ or $|l\rangle$ states) was introduced by taking a linear combination of the symmetry adapted $1\sigma_g$ and $1\sigma_u$ wavefunctions, $|r\rangle = (|1\sigma_g\rangle + |1\sigma_u\rangle)/\sqrt{2}$ and $|l\rangle = (|1\sigma_g\rangle - |1\sigma_u\rangle)/\sqrt{2}$. The full line at the lower right in figures 3(a)–(c) shows the prediction for the assumption of fully localized emission of the photoelectron from the doubly charged part of Ne_2 . It nicely resembles the asymmetric shape of the measured distribution, overestimating the total magnitude of the asymmetry. Figure 3(c) shows the same distribution with the dimer being oriented perpendicularly to the polarization axis of the photon beam. As expected, no left/right asymmetry is visible in that case, but a small up/down asymmetry, which is again overestimated by our calculations that imply complete localization.

As a next step we investigate the corresponding angular distribution for the ICD electron. Figure 4(a) shows the distribution for decay path A, figure 4(b) the one for decay channel B. Both angular distributions are—just as the one for the photoelectron—asymmetric with respect to the two atomic centres of the dimer. A striking difference is visible for the preferred direction of emission. While the ICD electron is emitted towards the Ne^{1+} for channel (A) it is emitted towards the Ne^{2+} in case of pathway (B). This implies the ICD electron being emitted from opposite sites in the two cases, which is exactly what one would intuitively expect from comparing the

two processes in figure 1. This finding maybe even more surprising, as the emitted ICD electron originates from a valence shell: for an excited/ionized van der Waals molecule valence electrons are often viewed as delocalized molecular orbitals.

In conclusion, the molecular frame angular distribution of photoelectrons and electrons from interatomic Coulombic decay are found to be strongly asymmetric for asymmetric breakup channels of Ne_2 . For the photoelectron this finding directly proves that a photon induced core hole in Ne_2 is best thought of as being localized. The observed asymmetry for the ICD electrons shows that in addition to the core hole also the $2s$ hole created by the Auger decay and the valence orbital that emits the ICD electron show strong features of localization.

Acknowledgments

This work was supported by BMBF, DFG, BESSY, JSPS and MEXT. We would like to express our thanks to Stefan Schramm and the staff at BESSY for excellent support during the beamtime. We are grateful also to S Stoychev, A Kuleff, B Averbukh and L S Cederbaum for stimulating discussion. KK and TW acknowledge support by DESY. XJL acknowledges support by JSPS.

References

- [1] Snyder L C 1971 *J. Chem. Phys.* **55** 95
- [2] Bagus P S 1972 *J. Chem. Phys.* **56** 224
- [3] Kintop J A, Machado W V M and Ferreira L G 1991 *Phys. Rev. A* **43** 3348
- [4] Thiel A, Schirmer J and Köppel H 2003 *J. Chem. Phys.* **119** 2088
- [5] Ehara M *et al* 2006 *J. Chem. Phys.* **124** 124311
- [6] Dill D *et al* 1978 *Phys. Rev. Lett.* **41** 1230
- [7] Matsumoto M *et al* 2006 *J. Phys. B: At. Mol. Opt. Phys.* **39** 375
- [8] Glans P *et al* 1996 *Phys. Rev. Lett.* **76** 2448
- [9] Rolles D *et al* 2005 *Nature* **437** 711
- [10] Björneholm O *et al* 2000 *Phys. Rev. Lett.* **84** 2826
- [11] Chen C T, Ma Y and Sette F 1989 *Phys. Rev. A* **40** 6737
- [12] Kosugi N 2003 *Chem. Phys.* **289** 117
- [13] Scheit S *et al* 2004 *J. Chem. Phys.* **121** 8393
- [14] Golovin A V *et al* 1997 *Phys. Rev. Lett.* **79** 4554
- [15] Saito N *et al* 2005 *J. Phys. B: At. Mol. Opt. Phys.* **38** L277
- [16] Adachi J *et al* 2007 *J. Phys. B: At. Mol. Opt. Phys.* **40** F285
- [17] Cederbaum L S, Zobeley J and Tarantelli F 1997 *Phys. Rev. Lett.* **79** 4778
- [18] Santra R and Cederbaum L S 2003 *Phys. Rev. Lett.* **90** 153401
Santra R and Cederbaum L S 2005 *Phys. Rev. Lett.* **94** 199901(E)
- [19] Pavlychev A A *et al* 1998 *Phys. Rev. Lett.* **81** 3623
- [20] Weber T *et al* 2001 *J. Phys. B: At. Mol. Opt. Phys.* **34** 3669
- [21] Poon H C and Tong S Y 1984 *Phys. Rev. B* **30** 6211
- [22] Santra R, Zobeley J and Cederbaum L S 2001 *Phys. Rev. B* **64** 245104
- [23] Jahnke T *et al* 2007 *Phys. Rev. Lett.* **99** 153401
- [24] Jahnke T *et al* 2004 *Phys. Rev. Lett.* **93** 083002
- [25] Ullrich J *et al* 2003 *Rep. Prog. Phys.* **66** 1463
- [26] Jagutzki O *et al* 2002 *Nucl. Instrum. Methods A* **477** 244
- [27] Weber T *et al* 2004 *Nature* **431** 437
- [28] Semenov S K *et al* 2000 *Phys. Rev. A* **61** 032704